

Positional-Scanning Combinatorial Libraries of Fluorescence Resonance Energy Transfer Peptides for Defining Substrate Specificity of the Angiotensin I-Converting Enzyme and Development of Selective C-Domain Substrates[†]

Patrícia A. Bersanetti,[‡] Maria Claudina C. Andrade,[§] Dulce E. Casarini,[§] Maria A. Juliano,[‡] Aloysius T. Nchinda,^{||} Edward D. Sturrock,^{||} Luiz Juliano,[‡] and Adriana K. Carmona^{*‡}

Department of Biophysics and Department of Medicine, Division of Nephrology, Escola Paulista de Medicina, Universidade Federal de São Paulo, Rua 3 de Maio 100, São Paulo 04044-020, Brazil, and Division of Medical Biochemistry, Institute of Infectious Disease and Molecular Medicine, University of Cape Town, Observatory 7925, Cape Town, South Africa

Received July 23, 2004; Revised Manuscript Received September 20, 2004

ABSTRACT: Positional-scanning combinatorial libraries of fluorescence resonance energy transfer peptides were used for the analyses of the S₃ to S₁' subsites of the somatic angiotensin I-converting enzyme (ACE). Substrate specificity of ACE catalytic domains (C- and N-domains) was assessed in an effort to design selective substrates for the C-domain. Initially, we defined the S₁ specificity by preparing a library with the general structure Abz-GXXZXK(Dnp)-OH [Abz = *o*-aminobenzoic acid, K(Dnp) = *N*^ε-2,4-dinitrophenyllsine, and X is a random residue], where Z was successively occupied with one of the 19 natural amino acids with the exception of Cys. The peptides containing Arg and Leu in the P₁ position had higher C-domain selectivity. In the sublibraries Abz-GXXRZK(Dnp)-OH, Abz-GXZRXX(Dnp)-OH, and Abz-GZXRXK(Dnp)-OH, Arg was fixed at P₁ so we could define the C-domain selectivity of the S₁', S₂, and S₃ subsites. On the basis of the results from these libraries, we synthesized peptides Abz-GVIRFK(Dnp)-OH and Abz-GVILFK(Dnp)-OH which contain the most favorable residues for C-domain selectivity. Systematic reduction of the length of these two peptides resulted in Abz-LFK(Dnp)-OH, which demonstrated the highest selectivity for the recombinant ACE C-domain ($k_{\text{cat}}/K_m = 36.7 \mu\text{M}^{-1} \text{s}^{-1}$) versus the N-domain ($k_{\text{cat}}/K_m = 0.51 \mu\text{M}^{-1} \text{s}^{-1}$). The substrate binding of Abz-LFK(Dnp)-OH with testis ACE using a combination of conformational analysis and molecular docking was examined, and the results shed new light on the binding characteristics of the enzyme.

The angiotensin I-converting enzyme (ACE,¹ EC 3.4.15.1) is a zinc-dipeptidyl carboxypeptidase that plays an important role in blood pressure regulation by converting the inactive decapeptide angiotensin I to the potent vasopressor angiotensin II (I). The enzyme is also able to hydrolyze bradykinin (2, 3) and other naturally occurring peptides such as substance P and luteinizing hormone-releasing hormone (4). Several ACE forms are present in mammalian tissues. A somatic isoform (150–180 kDa), which is expressed in endothelial, epithelial, and neuroepithelial cells, consists of

two homologous domains (N- and C-domains) within a single polypeptide sequence, each domain possessing its own catalytic site (5–8). A smaller isoenzyme (90–110 kDa), found exclusively in male germinal cells, contains a single active site and corresponds to the C-domain of the somatic enzyme with the exception of a short unique N-terminal sequence (9–11). The recent description of the crystal structure of human testis ACE provided new details at the molecular level (12). Another form of human ACE that consists of only the N-domain was found in ileal fluid of patients undergoing surgery and is believed to be a result of limited proteolysis of the parent somatic form (13).

ACE is primarily a membrane-bound protein, but a soluble form is found in many body fluids and is released from the cell surface by the action of a protein secretase or sheddase that cleaves the Arg1203–Ser1204 bond, 27 residues from the cell surface (14). The cytoplasmic domain of ACE is not necessary for sheddase recognition but is involved in modulation of ACE shedding (15).

The C- and N-domains of ACE are functional and share a high degree of homology, particularly at the active centers, but they differ in substrate specificities, inhibitor and chloride profiles (16–19), and their stability under denaturing conditions (20). The active sites of both domains cleave angiotensin I, substance P, and bradykinin with similar efficiency

[†] This work was supported by the Brazilian Agencies Fundação de Amparo a Pesquisa do Estado de São Paulo (FAPESP) and Conselho Nacional de Desenvolvimento Científico e Tecnológico (CNPq) and by the Wellcome Trust, U.K., and National Research Foundation.

* To whom correspondence should be addressed: Universidade Federal de São Paulo, Departamento de Biofísica, Rua Três de Maio 100, São Paulo 04044-020, SP Brazil. Telephone: 55-11-55764450. Fax: 55-11-55759617. E-mail: adriana@biofis.epm.br.

[‡] Department of Biophysics, Division of Nephrology, Escola Paulista de Medicina, Universidade Federal de São Paulo.

[§] Department of Medicine, Division of Nephrology, Escola Paulista de Medicina, Universidade Federal de São Paulo.

^{||} University of Cape Town.

¹ Abbreviations: ACE, angiotensin I-converting enzyme; Abz, *o*-aminobenzoic acid; CVFF, consistent valence force field; Dnp, 2,4-dinitrophenyl; ESFF, extensible systematic force field; FRET, fluorescence resonance energy transfer; MALDI-TOF, matrix-assisted laser desorption ionization time-of-flight; PS-SC, positional-scanning synthetic combinatorial.

(4), while the natural circulating tetrapeptide *N*-acetyl-seryl-aspartyl-lysyl-proline (21) and angiotensin 1–7 (Asp-Arg-Val-Tyr-Ile-His-Pro) (22) are more specific for the N-domain catalytic site. Selective inhibitors for each domain have already been described, such as the phosphinic peptide RXP407 (23) and RXPA380 (24), which have 1000- and 3000-fold higher inhibitor potencies for the N- and C-domains, respectively.

We have previously described fluorescence resonance energy transfer peptide analogues of the N-domain specific substrate *N*-acetyl-seryl-aspartyl-lysyl-proline (Ac-SDKP-OH) (25). The peptides Abz-SDK(Dnp)P-OH and Abz-TDK(Dnp)P-OH exhibited high N-domain selectivity, but were barely hydrolyzed by the C-domain (25). In the study presented here, we describe the development of selective substrates for the C-domain of ACE using positional-scanning synthetic combinatorial (PS-SC) libraries of fluorescence resonance energy transfer peptides. This strategy involves the successive replacement of each position in the peptide sequence with a single amino acid residue. Mixtures of amino acids are coupled to mixtures of resin-bound amino acids for the synthesis of the libraries. Besides some intrinsic limitations of the synthetic process, due to nonequimolar or incomplete libraries, the reported results using this approach for endoproteases seem to be very convincing (26–30). We synthesized a PS-SC library specially designed for screening peptidases with carboxydiptidase activity, where peptides contain the quencher group (Dnp) in the last position and a free C-terminal carboxyl group (31). Initially, we prepared a library with the general structure Abz-GXXZXK(Dnp)-OH [Abz = *o*-aminobenzoic acid, K(Dnp) = *N*^ε-2,4-dinitrophenyllysine, and X is a randomly incorporated residue], where the Z position was successively occupied with one of 19 amino acids with the exception of cysteine. To ensure equivalent coupling of the randomized residues, a balanced isokinetic mixture of 19 amino acids was used in the synthesis, as described previously (32). The selectivity of the S₁', S₂, and S₃ [nomenclature by Schechter and Berger (33)] subsites of ACE was examined with the sublibraries Abz-GXXRZK(Dnp)-OH, Abz-GXZRXX(Dnp)-OH, and Abz-GZXRXX(Dnp)-OH, in which Arg was fixed in the P₁ position because this was the optimal P₁ residue, in terms of domain selectivity, in the Abz-GXXZXK(Dnp)-OH library. The libraries were screened with wild-type recombinant human ACE and two full-length ACE mutants. On the basis of the library screen, we designed internally quenched substrates containing the most favorable residues that confer C-domain selectivity.

MATERIALS AND METHODS

Enzyme Preparation. Human testicular ACE was prepared as reported previously (14). The three human recombinant ACE proteins, namely, the wild type containing two intact functional domains and the two full-length ACE mutants containing only one intact catalytic site, were kindly supplied by F. Alhenc-Gelas from the Institut National de la Santé et de la Recherche Médicale (Paris, France). The molar concentrations of the enzymes were determined by active site titration with the tight-binding inhibitor lisinopril and analyzed as previously described (16).

Synthesis of Peptide Libraries. PS-SC libraries were synthesized by the methods previously described (28, 29), except Abz and Dnp were used as the fluorescence donor and acceptor, respectively. For preliminary experiments, we prepared a library with the general structure Abz-GXXZXK(Dnp)-OH, where the Z position was successively replaced with one of the 19 amino acids (cysteine excluded). X represents a randomly incorporated residue introduced by coupling a balanced mixture of 19 amino acids (31). Three other libraries were prepared with structures Abz-GXXRZK(Dnp)-OH, Abz-GXZRXX(Dnp)-OH, and Abz-GZXRXX(Dnp)-OH, in which two of the positions were fixed: the P₁ position as Arg and Z as P₁', P₂, and P₃ which included 19 naturally occurring amino acids with the other positions randomized (Cys excluded). Stock solutions of each peptide mixture were prepared in DMSO, and the concentrations were measured using the absorbance of Dnp, with a molar extinction coefficient ϵ_{365} of 17 300 M⁻¹ cm⁻¹.

Synthesis and Purification of Fluorescence-Quenched Peptides. The fluorescence resonance energy transfer peptides containing the Dnp group, coupled to the ϵ -NH₂ group of the ultimate Lys residue, were synthesized by a solid-phase methodology, using Fmoc-Lys(Dnp)-OH to introduce the quencher group (32). All the peptides obtained were purified by semipreparative HPLC. The molecular weight and purity of the synthesized peptides were checked by amino acid analysis and by molecular weight determination with MALDI-TOF mass spectrometry, using a ToFSpec E instrument from Micromass (Manchester, U.K.). The stock solutions of peptides were prepared in DMSO, and the concentrations were measured spectrophotometrically using the molar extinction coefficient of Dnp as described above.

Screening of Peptide Libraries. Hydrolysis of the peptide libraries was performed in 0.1 M Tris-HCl buffer (pH 7.0) containing 0.05 M NaCl and 10 μ M ZnCl₂. Enzymatic activity was continuously followed at 37 °C in a Hitachi F-2000 fluorimeter by measuring the fluorescence at 420 nm (λ_{em}) and 320 nm (λ_{ex}). The assays were performed at low substrate concentrations ($[S] \ll K_m$), and the initial velocity of hydrolysis was measured. Under these conditions, the velocity is proportional to the catalytic efficiency, k_{cat}/K_m (29).

Determination of Kinetic Parameters for Peptides Derived from the Libraries. Assays with peptides derived from the libraries were performed at 37 °C, in 0.1 M Tris-HCl (pH 7.0) containing 0.05 M NaCl and 10 μ M ZnCl₂. Enzymatic activity was continuously followed in a Hitachi F-2000 fluorimeter by measuring the fluorescence at 420 nm (λ_{em}) and 320 nm (λ_{ex}). The enzyme concentration for the initial rate determination was chosen so that less than 5% of the substrate present was hydrolyzed. The slope was converted into micromoles of substrate hydrolyzed per minute based on a calibration curve obtained from complete hydrolysis of each peptide. The inner-filter effect was corrected using an empirical equation as previously described (25). The kinetic parameters K_m and k_{cat} were calculated by the nonlinear regression data analysis *Grafit* program (34). The k_{cat}/K_m values were calculated as the ratio of these two parameters.

Optimum pH and Chloride Influence on Catalytic Activity. The pH dependence of ACE hydrolysis using the substrate Abz-LFK(Dnp)-OH (10 μ M) was studied over a pH range of 5.0–9.5. We used a four-component buffer comprised of

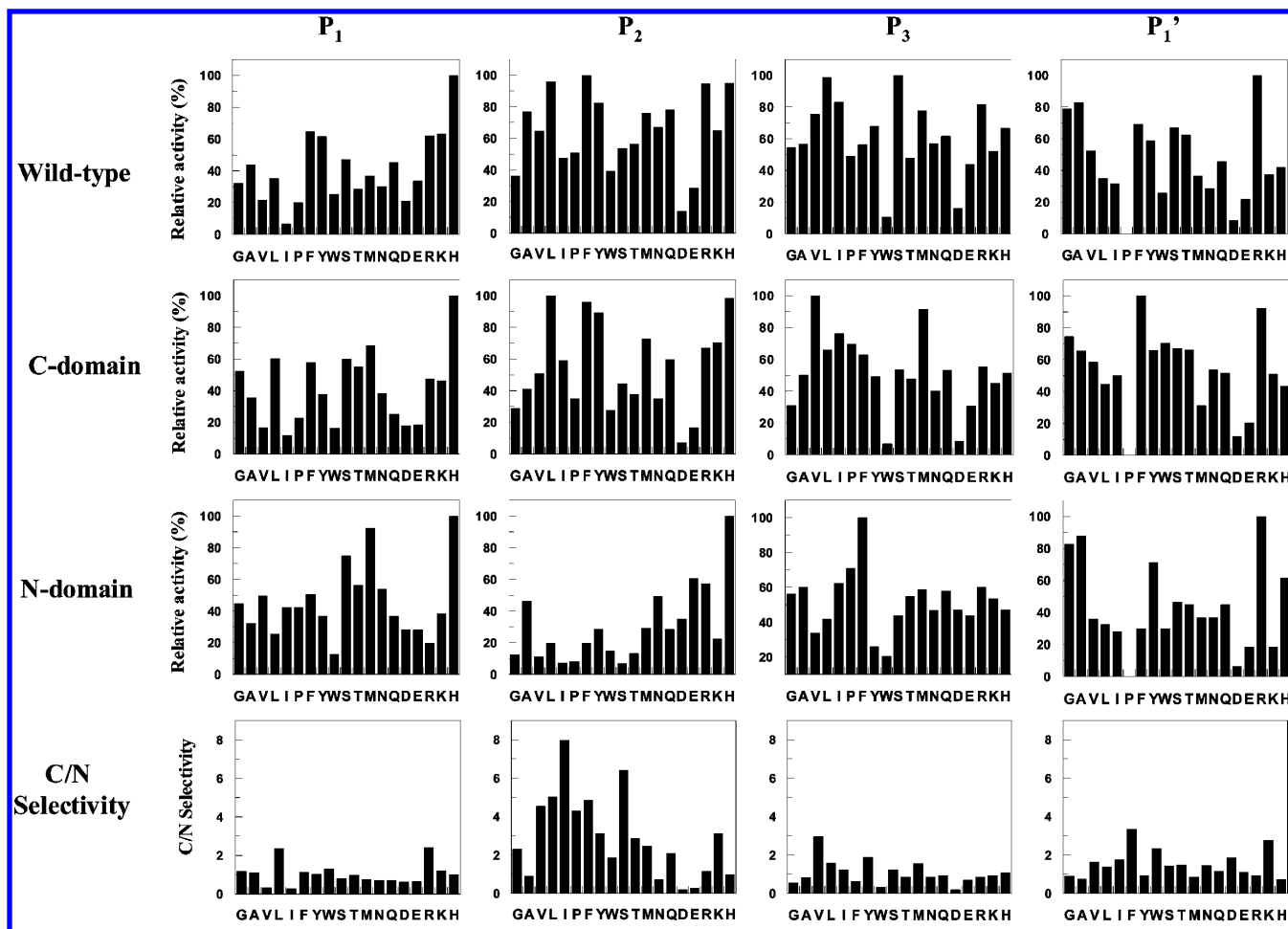


FIGURE 1: Combinatorial fluorescence-quenched peptide libraries for scanning of subsites P_3 – P_1' . The libraries with Abz-GXXZXX(Dnp)-OH (P_1), Abz-GXZRXX(Dnp)-OH (P_2), Abz-GZXRXX(Dnp)-OH (P_3), and Abz-GXXRZK(Dnp)-OH (P_1') general sequences were incubated with the wild type, the C-domain, and the N-domain of ACE as described in Materials and Methods. The assays were performed at low substrate concentrations where the reactions followed first-order conditions. The y axis provides the relative catalytic efficiency values (%) normalized by the best substrate in each series. The x axis shows the amino acids in the different P_3 – P_1' positions that were investigated. The errors were less than 5% for any obtained value. According to Schechter and Berger (33) P_1 – P_3 are designed for amino acid residues in the N-terminal direction and P_1' is designed for residues in the C-terminal direction from the scissile bond.

25 mM glycine, 25 mM acetic acid, 25 mM Mes, and 75 mM Tris in the presence of 100 mM NaCl and 10 μ M ZnCl₂. Enzymatic activity was measured at 37 °C, using the fluorimetric assay described above.

The influence of chloride ions (0–500 mM) on the catalytic activity of recombinant forms of ACE was investigated. The enzyme was incubated with Abz-LFK(Dnp)-OH (10 μ M) at 37 °C in 0.05 M HEPES (pH 7.6) containing 10 μ M ZnCl₂. The hydrolysis was followed by the continuous fluorimetric assay described above.

Determination of the Substrate Cleavage Site. The scissile bonds of hydrolyzed peptides were identified by isolation of the fragments using analytical HPLC (as described above), and their structures were deduced from amino acid sequencing (protein sequencer PPSQ-23, Shimadzu, Tokyo, Japan) and by MALDI-TOF mass spectrometry.

Modeling Studies. Molecular modeling calculations were performed using the DISCOVER module of INSIGHT II (version 98.0, Accelrys Inc.) on a Silicon Graphics Octane 1 workstation. The starting structure was the X-ray crystal structure of testis ACE complexed with a known inhibitor lisinopril (12). After the crystallographic water molecules had been removed and hydrogens added, the CVFF and the

ESFF (metal adapted) force fields (35) were used in all energy minimizations and dynamic runs. The conjugate gradient minimization algorithm was used after running 1000 initial steps, and then 3000 cycles of molecular dynamics followed by 3000 cycles of energy minimization in an NTV ensemble, at a temperature of 300 K. All calculations were carried out with a dielectric constant of 1.00 and a cutoff distance of 9.50 Å. The structure of Abz-LFK(Dnp)-OH was generated with standard bond lengths and angles using the builder tool of INSIGHT II (Accelrys Inc.) and then minimized. The initial position of Abz-LFK(Dnp)-OH in the active site of the catalytic C-domain of ACE was determined by superimposing the important pharmacophoric groups of the Abz-LFK(Dnp)-OH inhibitor on the corresponding atoms of lisinopril in the ACE–lisinopril complex. After removal of the reference inhibitor (lisinopril), the structure of the C-domain–Abz-LFK(Dnp)-OH complex was refined by running an energy minimization and molecular dynamics.

RESULTS

C-Domain Selectivity Defined by Peptide Libraries. PS-SC libraries were used to map the P_3 – P_1' substrate specificity of wild-type ACE and two mutants, each containing only

Table 1: Kinetic Parameters for the Hydrolysis of FRET Peptides by Recombinant Forms of ACE^a

peptide	wild type			C-domain			N-domain		
	k_{cat} (s ⁻¹)	K_m (μM)	k_{cat}/K_m ($\mu\text{M}^{-1} \text{s}^{-1}$)	k_{cat} (s ⁻¹)	K_m (μM)	k_{cat}/K_m ($\mu\text{M}^{-1} \text{s}^{-1}$)	k_{cat} (s ⁻¹)	K_m (μM)	k_{cat}/K_m ($\mu\text{M}^{-1} \text{s}^{-1}$)
Abz-GVIRFK(Dnp)-OH	11.9	0.35	34.0	19.6	0.38	51.8	2.0	0.52	3.8
Abz-GVILFK(Dnp)-OH	22.4	1.00	22.4	37.9	0.58	65.4	9.4	3.14	3.0
Abz-VIRFK(Dnp)-OH	13.8	0.43	32.1	8.7	0.36	24.1	0.9	0.45	2.0
Abz-VILFK(Dnp)-OH	26.3	0.96	27.4	18.0	0.95	18.9	1.2	1.01	1.2
Abz-IRFK(Dnp)-OH	14.6	0.44	32.8	10.4	0.40	25.9	5.0	2.63	1.9
Abz-ILFK(Dnp)-OH	75.6	1.44	32.0	62.6	2.04	30.7	10.2	6.29	1.6
Abz-RFK(Dnp)-OH	62.1	3.68	16.9	64.7	2.94	22.0	3.2	5.93	0.6
Abz-LFK(Dnp)-OH	82.6	3.98	20.8	80.8	2.20	36.7	3.9	7.74	0.5

^a The assays were performed at 37 °C in 0.1 M Tris-HCl (pH 7.0) containing 0.05 M NaCl and 10 μM ZnCl₂. Measurements were made as described in Materials and Methods. The standard deviations of the kinetic constants were less than 5%.

one functional catalytic site, termed the C-domain and N-domain. Initially, the library with the general sequence Abz-GXXZXK(Dnp)-OH was scanned to define the specificity of the P₁ position. Figure 1 shows the relative values normalized by the residue with the higher velocity of the hydrolysis value. The ratio of the relative velocity values for the C-domain versus the N-domain (C/N selectivity) indicates the residues that favor C-domain selectivity (Figure 1). All three forms of ACE showed a preference for His in the P₁ position. The relative activities of Leu and Arg were ~2- and ~3-fold higher, respectively, for the C-domain. Peptides containing Leu at P₁ were very susceptible to hydrolysis by the C-domain, but poorly hydrolyzed by the N-domain. Surprisingly, the sequences containing Ile at P₁ were almost resistant to hydrolysis by both the wild type and the C-domain and poorly hydrolyzed by the N-domain. The peptides containing Tyr and Phe were efficiently hydrolyzed by the three forms of ACE, while those containing Trp at P₁ gave the lowest relative activity of the aromatic amino acids. Met was also readily accommodated by both active sites, being slightly better for the N-domain.

The three other sublibraries with the general sequences Abz-GXXRZK(Dnp)-OH, Abz-GXZRXX(Dnp)-OH, and Abz-GZXRXX(Dnp)-OH were screened to study the S₁' , S₂, and S₃ specificities, respectively. In these sequences, Arg was fixed in the P₁ position due to its C-domain preference and also to increase the water solubility of the libraries.

Figure 1 shows that the S₂ subsite of the C-domain accommodated a broad range of amino acids while the N-domain was more restrictive. His at position P₂ gave the highest relative activity for the three forms of ACE. Arg gave similar results for both active sites, while Lys was 3-fold better in the case of the C-domain. In contrast, peptides containing Asp and Glu at position P₂ were poorly hydrolyzed by the C-domain, but were better substrates for the N-domain. The highest C/N selectivity values determined among all the substrates that were tested were presented by the peptides with Ile (8-fold) and Ser (6-fold) at P₂.

The S₃ subsite of the C-domain and of wild-type ACE presented very similar hydrolysis profiles, while the N-domain showed somewhat different preferences. The main contrasts were observed with the substrates containing hydrophobic aromatic or aliphatic amino acids in the P₃ position. Substrates with Phe at P₃ were better hydrolyzed by the N-domain than by the C-domain; Tyr was more susceptible to hydrolysis by the C-domain, and Trp was the poorest residue for both active sites. A clear preference for

substrates containing Val at P₃ was observed for the C-domain.

Not surprisingly, the S₁' subsite presented a strict restriction for Pro with the sequence Abz-GXXRPK(Dnp)-OH being resistant to hydrolysis by all three recombinant forms of ACE. This result validated the use of these combinatorial libraries in the study of the substrate specificities of carboxydipeptidases. Again, the main differences in the specificity of the sites could be observed with the aromatic residues. Substrates with Phe followed by Trp at P₁' were more susceptible to hydrolysis by the C-domain than by the N-domain, while peptides with Tyr in this position were better substrates for the N-domain active site. With the exception of Lys, which was almost 3-fold more selective for the C-domain, the other residues in the P₁' position gave similar relative activities for both active sites.

ACE Activity on Substrates Designed from the Results for the Libraries. The results from the peptide libraries were used to design selective substrates for the C-domain by incorporating the best amino acids in each subsite (S₃ to S₁'). The fluorescence resonance energy transfer peptides Abz-GVIRFK(Dnp)-OH and Abz-GVILFK(Dnp)-OH were prepared and assayed with human wild-type recombinant ACE and its functional C- and N-domains (Table 1). Shorter homologues were also prepared, and the ratio of the catalytic efficiency, C- versus N-domain, increased with the reduction of the length of the peptide (Figure 2), mainly due to the higher k_{cat} values (Table 1). The k_{cat} for the hydrolysis of the tripeptide Abz-LFK(Dnp)-OH by the C-domain was 20 times higher than that for the N-domain. For the hexapeptide AbzGVILFK(Dnp), the k_{cat} was only 4-fold higher for the C-domain (Table 1). This series of substrates was also tested with purified human testis ACE. The kinetic parameters presented in Table 2, similar to those for the recombinant C-domain, demonstrated that the shortening of the length of the peptide increased the k_{cat} values but reduced the substrate's affinity as reflected by the higher K_m value. All the peptides that were tested were cleaved at the Xaa-Phe bond by the recombinant forms as well as testis ACE.

Effects of pH and Chloride Concentration. The effect of pH on the hydrolysis of Abz-LFK(Dnp)-OH by the recombinant N- and C-domains was determined over the pH range of 5.0–9.5 (Figure 3). Optimal hydrolysis occurred around pH 7.5 for the N-domain and pH 8.0 for the C-domain. The bell-shaped curves are characteristic of those reported for ACE substrates. Abz-LFK(Dnp)-OH was hydrolyzed by the N-domain over a broader pH range (6.0–9.0). In the acidic

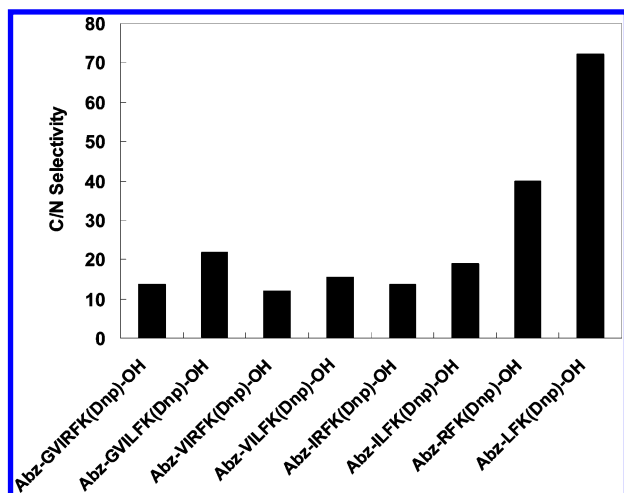


FIGURE 2: Efficacy of the ACE domains in the hydrolysis of the synthetic substrates derived from the peptide libraries. Efficacy C/N is the ratio of recombinant C-domain k_{cat}/K_m vs recombinant N-domain k_{cat}/K_m values.

Table 2: Kinetic Parameters for the Hydrolysis of FRET Peptides Containing the Most Favorable Residues for the C-Domain with Testis ACE^a

peptide	k_{cat} (s ⁻¹)	K_m (μ M)	k_{cat}/K_m (μ M ⁻¹ s ⁻¹)
Abz-GVIRFK(Dnp)-OH	14.8	0.72	20.5
Abz-GVILFK(Dnp)-OH	20.6	1.30	15.9
Abz-VIRFK(Dnp)-OH	10.4	0.48	21.7
Abz-VILFK(Dnp)-OH	7.3	0.64	11.4
Abz-IRFK(Dnp)-OH	7.5	0.70	10.7
Abz-ILFK(Dnp)-OH	34.3	1.42	24.1
Abz-RFK(Dnp)-OH	48.2	3.40	14.2
Abz-LFK(Dnp)-OH	56.1	3.43	16.5

^a Conditions of hydrolysis are as described in the footnote of Table 1. The standard deviations of the kinetic constants were less than 5%.

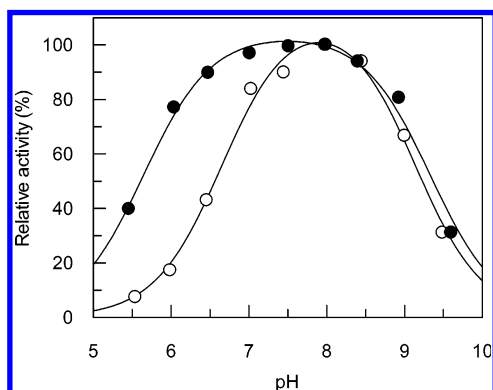


FIGURE 3: pH dependence of Abz-LFK(Dnp)-OH hydrolysis by recombinant forms of ACE: C-domain (○) and N-domain (●). The hydrolysis conditions are described in Materials and Methods.

limb, the pK_a determined for the N-domain was 5.7 and for the C-domain 6.7.

The chloride anion concentration had a greater effect on the catalytic activity of the recombinant ACE C-domain with Abz-LFK(Dnp)-OH, as shown in Figure 4. The N-domain reached maximum activity with 0.05 M NaCl while the C-domain with 0.1 M chloride. In these assays of optimal pH and salt determination, a concentration of the recombinant N-domain 50-fold higher than that of the C-domain was used to obtain measurable fluorescence values.

Modeling of Abz-LFK(Dnp)-OH. The substrate Abz-LFK(Dnp)-OH, which presented the highest C-domain selectivity,

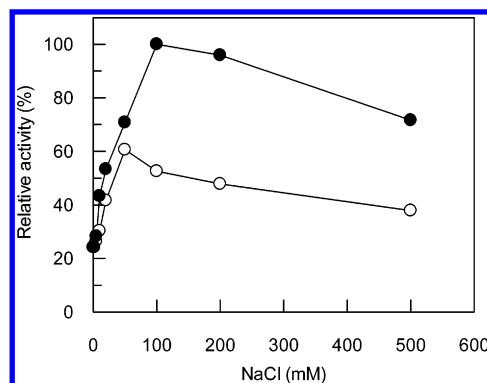


FIGURE 4: Effect of NaCl on Abz-LFK(Dnp)-OH hydrolysis by recombinant forms of ACE: C-domain (●) and N-domain (○).

was modeled into the testis ACE binding site occupying the S_1 , S_1' , and S_2' subsites (Figure 5A). From the docking experiments, the energy-minimized bound conformer of Abz-LFK(Dnp)-OH in the active site of the C-domain was obtained. The total potential energy of the protein–ligand interaction was found to be -778.8 kcal/mol, which is an indication of the relative stability of the enzyme–ligand complex. The residues forming the subsites of the C-domain active site were defined as those located less than 6.00 Å from the important functionalities of Abz-LFK(Dnp)-OH. The numbers of critical residues in the C-domain are according to Natesh et al. (12), and in parentheses are shown the corresponding residues in the somatic ACE (7). The modeling revealed that the isopropyl chain of the P_1 leucine interacts with the hydrophobic Val518 (Val1094) and the polar Ser516 (Ser1092) of the S_1 subsite at distances of 2.25 and 4.95 Å, respectively. The distance between the Leu carbonyl and the Zn atom in the active site of the C-domain was observed to be 5.63 Å. This value is larger than expected, but is probably due to the fact that the docking experiment was performed in the absence of crystallographic water. The P_1' phenylalanine interacts with residues Glu162 (Glu738), Thr166 (Thr742), Gln281 (Gln857), Asp377 (Asp953), and Val380 (Val956) (Figure 5B). In the N-domain, Glu162 (Glu738) and Asp377 (Asp953) are replaced with Asp and Gln, respectively. Thus, these interactions are likely to contribute to the domain selectivity of this substrate. The S_2' subsite readily accommodates the lysine-Dnp residue of the Abz-LFK(Dnp)-OH substrate. Thr282 (Thr858) and Asp453 (Asp1029), residues that are not conserved in the N- and C-domains, make contact with the phenyl ring of the dinitrophenyl group. The Abz-LFK(Dnp)-OH substrate was also docked with a homology model of the N-domain (36). However, the calculated binding energy for the N-domain–substrate complex was significantly higher than that for the C-domain complex, indicating that the latter is a more stable complex. Moreover, less than 40% of the C-domain residues' N-domain counterparts made contact with the Abz-LFK(Dnp)-OH substrate.

DISCUSSION

Recent findings confirm that the physiological functions of ACE are not limited to the cardiovascular system, and this has awakened an interest in defining the role of the enzyme and, more specifically, its N- and C-domain active sites in different biological processes. Rousseau et al. (21) showed that the natural circulating tetrapeptide involved in

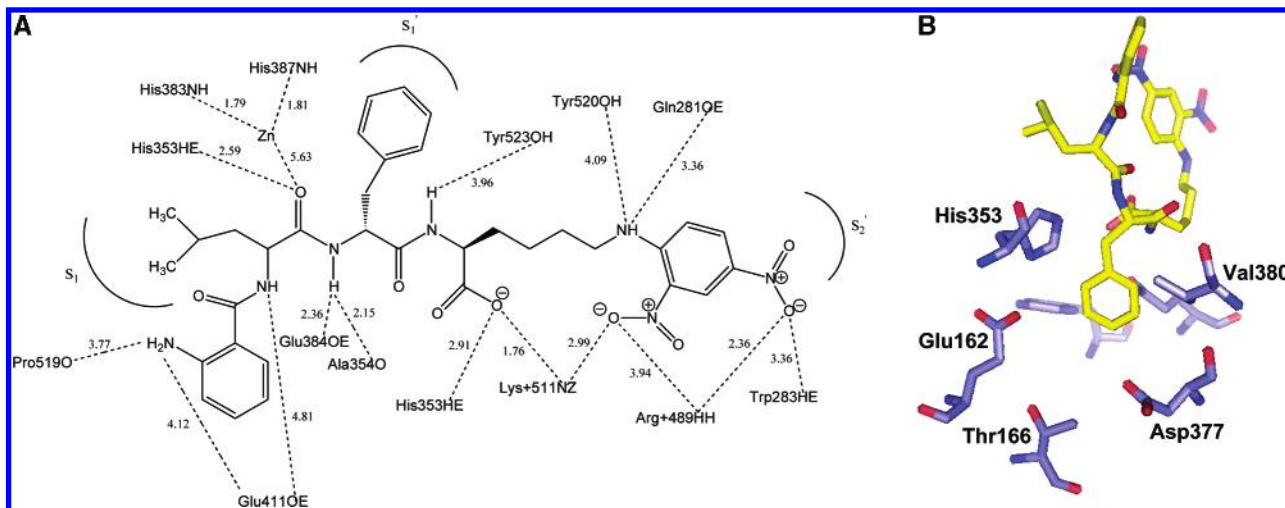


FIGURE 5: Schematic representation of Abz-LFK(Dnp)-OH modeled into the active site of testis ACE. (A) Different binding subsites and the Abz-LFK(Dnp)-OH peptide residues that make contact with the active site by hydrogen bonding (dashed lines). (B) Interactions between the P₁' Phe (yellow) and S₁' subsite residues (blue).

the control of hematopoietic stem cell proliferation, *N*-acetylseryl-aspartyl-lysyl-proline (Ac-SDKP-OH), was a specific substrate for the N-domain of ACE. Furthermore, the peptide angiotensin 1–7 is also an N-domain specific substrate and a C-domain selective inhibitor (22). We have previously described a rapid and sensitive method for assaying ACE activity using fluorescence resonance energy transfer substrates with the general structure Abz-peptidyl-K(Dnp)P-OH (25). In addition, specific substrates for the N-domain were developed. The peptides Abz-SDK(Dnp)P-OH and Abz-TDK(Dnp)P-OH are hydrolyzed by the N-domain with k_{cat} values 250–300 times higher than those obtained for the C-domain. Michaud et al. (37) mapped the specificity of the ACE S₃–S₁' subsites by using a series of synthetic substrates based on the Ac-SDKP-OH structure. They defined some of the C-domain preferences and demonstrated that shortening of the peptidic chain increased this active site specificity. However, a systematic study of the requirements of the ACE domains has never been performed. For this purpose, we developed PS-SC fluorogenic peptide libraries that allowed us to evaluate the substrate specificity of the two active sites of ACE and to define the requirements for C-domain selectivity. We mapped the S₃ to S₁' subsites of wild-type ACE, containing two intact functional domains, and two full-length ACE mutants, each containing only one intact catalytic site. Comparative analysis of the specificity of both active sites elicited the residues that favor C-domain selectivity (Figure 1). The peptide Abz-LFK(Dnp)-OH was the most selective substrate for the C-domain of ACE.

The pH profile for the hydrolysis of this peptide by the N- and C-domains demonstrated that optimal activity for both forms of the enzyme occurred around pH 7.5 and the curves were bell-shaped (Figure 3). However, the N-domain hydrolyzed this peptide over a broader pH range and with very low catalytic efficiency.

We observed a stronger NaCl dependence for the hydrolysis of Abz-LFK(Dnp)-OH by the C-domain than by the N-domain (Figure 4). This is a feature observed for some natural ACE substrates (1, 3, 17).

Testis ACE followed the same pattern of hydrolysis presented by the recombinant ACE C-domain, but cleaved the peptides with lower k_{cat} values and thus catalytic

efficiencies (k_{cat}/K_m). However, the hydrolysis of Abz-FRK-(Dnp)P-OH ($k_{\text{cat}}/K_m = 20.5 \mu\text{M}^{-1} \text{s}^{-1}$) and Abz-YRK(Dnp)P-OH ($k_{\text{cat}}/K_m = 25.5 \mu\text{M}^{-1} \text{s}^{-1}$) by testis ACE is stronger or similar to that of the recombinant C-domain. Araujo et al. (25) determined these values for the hydrolysis of Abz-FRK-(Dnp)P-OH and Abz-YRK(Dnp)P-OH by the recombinant C-domain to be 25.6 and 12.5 $\mu\text{M}^{-1} \text{s}^{-1}$, respectively.

Molecular docking of the energy-minimized conformer of Abz-LFK(Dnp)-OH in the testis ACE active site provides a clearer understanding of a possible molecular basis for the substrate's domain specificity. The bulky aromatic ring of the Phe at P₁' extends into the deep S₁' pocket (Figure 5B). Of the residues that make contact with the P₁' residue, Glu162 and Glu376 are both replaced with a smaller Asp in the N-domain. This substitution increases the size of the S₁' pocket which would favor a Tyr at P₁' as opposed to Phe. On the other hand, the Asp377 to Gln substitution would affect the charge of this region and could interact with the hydroxyl group of a tyrosine which we have shown to be a preferred P₁' residue for N-domain hydrolysis (Figure 1). Finally, Val380 which displays a hydrophobic interaction with the aryl Phe is replaced with the more hydrophilic Thr. The testis ACE Ser516 in the S₁ pocket is replaced with an asparagine in the N-domain. The less polar hydroxyl group favors the isopropyl P₁ group of the Leu. Furthermore, Ser516 is more likely to make contact with Lys and Arg which exhibited greater C-domain selectivity. Similarly, the Val518 to Thr substitution also affects the hydrophobicity of the S₁ subsite. The hydrophobic interactions with the S₂' pocket might be important for C-domain inhibitor selectivity as reported previously (38). However, more recently, Georgiadis et al. (39) have suggested that the orientation of the hydrophobic P₂' residue is more important for C-domain specificity. In the case of Abz-LFK(Dnp)-OH, it is unlikely that the lysine confers any selectivity per se as replacement of this P₂' residue with other groups does not have a significant effect on the C-domain selectivity (A. K. Carmona et al., unpublished data).

In conclusion, we provide a detailed description of the substrate specificity of both active sites of somatic ACE and have characterized differences that better define the C-domain's preference for certain substrates. In addition, we

have developed C-domain selective substrates that will facilitate further characterization of this active site as well as the development of domain specific inhibitors.

REFERENCES

- Skeggs, L. T., Kahn, J. R., and Shumway, N. P. (1956) The preparation and function of the hypertensin-converting enzyme, *J. Exp. Med.* 103, 295–299.
- Yang, H. Y. T., Erdős, E. G., and Levin, Y. (1970) A dipeptidyl carboxypeptidase that converts angiotensin I and inactivates bradykinin, *Biochim. Biophys. Acta* 214, 374–376.
- Dorer, F. E., Kahn, J. R., Lentz, K. E., Levine, M., and Skeggs, L. T. (1974) Hydrolysis of bradykinin by angiotensin-converting enzyme, *Circ. Res.* 34, 824–827.
- Jaspard, E., Wei, L., and Alhenc-Gelas, F. (1993) Differences in the properties and enzymatic specificities of the two active sites of angiotensin I-converting enzyme (kininase II). Studies with bradykinin and other natural peptides, *J. Biol. Chem.* 268, 9496–9503.
- Hubert, C., Houot, A. M., Corvol, P., and Soubrier, F. (1991) Structure of the angiotensin I-converting enzyme gene. Two alternate promoters correspond to evolutionary steps of a duplicated gene, *J. Biol. Chem.* 266, 15377–15383.
- Kumar, R. S., Thekkumkara, T. J., and Sen, G. C. (1991) The mRNAs encoding the two angiotensin-converting isozymes are transcribed from the same gene by a tissue-specific choice of alternative transcription initiation sites, *J. Biol. Chem.* 266, 3854–3862.
- Soubrier, F., Alhenc-Gelas, F., Hubert, C., Allegrini, J., John, M., Tregear, G., and Corvol, P. (1988) Two putative active centers in human angiotensin I-converting enzyme revealed by molecular cloning, *Proc. Natl. Acad. Sci. U.S.A.* 85, 9386–9390.
- Bernstein, K. E., Martin, B. M., Edwards, A. S., and Bernstein, E. A. (1989) Mouse angiotensin-converting enzyme is a protein composed of two homologous domains, *J. Biol. Chem.* 264, 11945–11951.
- Lattion, A.-L., Soubrier, F., Allegrini, J., Hubert, C., Corvol, P., and Alhenc-Gelas, F. (1989) The testicular transcript of the angiotensin I-converting enzyme encodes for the ancestral, non-duplicated form of the enzyme, *FEBS Lett.* 252, 99–104.
- Ehlers, M. R. W., Fox, E. A., Strydom, D. J., and Riordan, J. F. (1989) Molecular cloning of human testicular angiotensin-converting enzyme: the testis isozyme is identical to the C-terminal half of endothelial angiotensin-converting enzyme, *Proc. Natl. Acad. Sci. U.S.A.* 86, 7741–7745.
- Kumar, R. S., Kusari, J., Roy, S. N., Soffer, R. L., and Sen, G. C. (1989) Structure of testicular angiotensin-converting enzyme. A segmental mosaic isozyme, *J. Biol. Chem.* 264, 16754–16758.
- Natesh, R., Schwager, S. L. U., Sturrock, E. D., and Acharya, K. R. (2003) Crystal structure of the human angiotensin-converting enzyme-lisinopril complex, *Nature* 421, 551–554.
- Deddish, P. A., Wang, J., Michel, B., Morris, P. W., Davidson, N. O., Skidgel, R. A., and Erdős, E. G. (1994) Naturally occurring active N-domain of human angiotensin I-converting enzyme, *Proc. Natl. Acad. Sci. U.S.A.* 91, 7807–7811.
- Woodman, Z. L., Oppong, S. Y., Cook, S., Hooper, N. M., Schwager, S. L. U., Brandt, W. F., Ehlers, M. R. W., and Sturrock, E. D. (2000) Shedding of somatic angiotensin-converting enzyme (ACE) is inefficient compared with testis ACE despite cleavage at identical stalk sites, *Biochem. J.* 347, 711–718.
- Chubb, A. J., Schwager, S. L. U., Merwe, E. V., Ehlers, M. R. W., and Sturrock, E. D. (2004) Deletion of the cytoplasmic domain increases basal shedding of angiotensin-converting enzyme, *Biochem. Biophys. Res. Commun.* 314, 971–975.
- Ehlers, M. R. W., and Riordan, J. F. (1991) Angiotensin-converting enzyme: zinc- and inhibitor-binding stoichiometries of the somatic and testis isozymes, *Biochemistry* 30, 7118–7126.
- Wei, L., Alhenc-Gelas, F., Corvol, P., and Clauser, E. (1991) The two homologous domains of human angiotensin I-converting enzyme are both catalytically active, *J. Biol. Chem.* 266, 9002–9008.
- Deddish, P. A., Jackman, H. L., Skidgel, R. A., and Erdos, E. G. (1997) Differences in the hydrolysis of enkephalin congeners by the two domains of angiotensin converting enzyme, *Biochem. Pharmacol.* 53, 1459–1463.
- Wei, L., Clauser, E., Alhenc-Gelas, F., and Corvol, P. (1992) The two homologous domains of human angiotensin I-converting enzyme interact differently with competitive inhibitors, *J. Biol. Chem.* 267, 13398–13405.
- Voronov, S., Zueva, N., Orlov, V., Arutyunyan, A., and Kost, O. (2002) Temperature-induced selective death of the C-domain within angiotensin-converting enzyme molecule, *FEBS Lett.* 522, 77–82.
- Rousseau, A., Michaud, A., Chauvet, M.-T., Lenfant, M., and Corvol, P. (1995) The hemoregulatory peptide N-acetyl-Ser-Asp-Lys-Pro is a natural and specific substrate of the N-terminal active site of human angiotensin-converting enzyme, *J. Biol. Chem.* 270, 3656–3661.
- Deddish, P. A., Marcic, B., Jackman, H. L., Wang, H. Z., Sikgel, R. A., and Erdős, E. G. (1998) N-Domain-specific substrate and C-domain inhibitors of angiotensin-converting enzyme: angiotensin-(1–7) and keto-ACE, *Hypertension* 31, 912–917.
- Dive, V., Cotton, J., Yiotakis, A., Michaud, A., Vassiliou, S., Jiracek, J., Vazeux, G., Chauvet, M. T., Cuniassé, P., and Corvol, P. (1999) RXP 407, a phosphinic peptide, is a potent inhibitor of angiotensin I converting enzyme able to differentiate between its two active sites, *Proc. Natl. Acad. Sci. U.S.A.* 96, 4330–4335.
- Georgiadis, D., Beau, F., Czarny, B., Cotton, J., Yiotakis, A., and Dive, V. (2003) Roles of the two active sites of somatic angiotensin-converting enzyme in the cleavage of angiotensin I and bradykinin: insights from selective inhibitors, *Circ. Res.* 93, 148–154.
- Araujo, M. C., Melo, R. L., Cesari, M. H., Juliano, M. A., Juliano, L., and Carmona, A. K. (2000) Peptidase specificity characterization of C- and N-terminal catalytic sites of angiotensin I-converting enzyme, *Biochemistry* 39, 8519–8525.
- Rano, T. A., Timkey, T., Peterson, E. P., Rotonda, J., Nicholson, D. W., Becker, J. W., Chapman, K. T., and Thornberry, N. A. (1997) A combinatorial approach for determining protease specificities: application to interleukin-1 β converting enzyme (ICE), *Chem. Biol.* 4, 149–155.
- Thornberry, N. A., Rano, T. A., Peterson, E. P., Rasper, D. M., Timkey, T., Garcia-Calvo, M., Houtzager, V. M., Nordstrom, P. A., Roy, S., Vaillancourt, J. P., Chapman, K. T., and Nicholson, D. W. (1997) A combinatorial approach defines specificities of members of the caspase family and granzyme B. Functional relationships established for key mediators of apoptosis, *J. Biol. Chem.* 272, 17907–17911.
- Harris, J. L., Backes, B. J., Leonetti, F., Mahrus, S., Ellman, J. A., and Craik, C. S. (2000) Rapid and general profiling of protease specificity by using combinatorial fluorogenic substrate libraries, *Proc. Natl. Acad. Sci. U.S.A.* 97, 7754–7759.
- Backes, B. J., Harris, J. L., Leonetti, F., Craik, C. S., and Ellman, J. A. (2000) Synthesis of positional-scanning libraries of fluorogenic peptide substrates to define the extended substrate specificity of plasmin and thrombin, *Nat. Biotechnol.* 18, 187–193.
- Herman, L. W., Tarr, G., and Kates, S. A. (1996) Optimization of the synthesis of peptide combinatorial libraries using a one-pot method, *Mol. Diversity* 2, 147–155.
- Cotrin, S. S., Puzer, L., Judice, W. A. S., Carmona, A. K., Juliano, L., and Juliano, M. A. (2004) Positional-scanning combinatorial libraries of fluorescence resonance energy transfer (FRET) peptides to define substrate specificity of carboxidipeptidases: Assays with human cathepsins B, *Anal. Biochem.* 335, 244–252.
- Barlos, K., Gatos, D., Rapolos, S., Papaphotiu, G., Schafer, W., and Yao, W. Q. (1989) Esterification of partially protected peptide-fragments with resins: utilization of 2-chlorotriethylchloride for synthesis of leu-15-gastrin-I, *Tetrahedron Lett.* 30, 3947–3950.
- Schechter, I., and Berger, A. (1967) On the size of the active site in proteases. I. Papain, *Biochem. Biophys. Res. Commun.* 27, 157–162.
- Leatherbarrow, R. J. (1992) *Grafit*, version 5.0, Erithacus Software Ltd., Staines, U.K.
- www.accelrys.com/support/life/discover/force-field/esfSBL.html.
- Acharya, K. R., Riordan, J. F., Sturrock, E. D., and Ehlers, M. R. W. (2003) Angiotensin-converting enzyme: A new target for structure-based drug design, *Nat. Rev. Drug Discovery* 2, 891–902.
- Michaud, A., Chauvet, M. T., and Corvol, P. (1999) N-Domain selectivity of angiotensin I-converting enzyme as assessed by structure–function studies of its highly selective substrate, *N-*

- acetyl-seryl-aspartyl-lysyl-proline, *Biochem. Pharmacol.* 57, 611–618.
38. Perich, R. B., Jackson, B., and Johnston, C. I. (1994) Structural constraints of inhibitors for binding at two active sites on somatic angiotensin converting enzyme, *Eur. J. Pharmacol.* 266, 201–211.
39. Georgiadis, D., Cuniasse, P., Cotton, J., Yiotakis, A., and Dive, V. (2004) Structural determinants of RXPA380, a potent and highly selective inhibitor of the angiotensin-converting enzyme C-domain, *Biochemistry* 43, 8048–8054.

BI048423R